

Can Non-Linear Elasticity Explain Contact-Line Roughness at Depinning?

Pierre Le Doussal¹, Kay Jörg Wiese¹, Elie Raphael² and Ramin Golestanian³

¹CNRS-Laboratoire de Physique Théorique de l'Ecole Normale Supérieure, 24 rue Lhomond 75005 Paris, France

²Laboratoire de Physique de la Matière Condensée, Collège de France, 11 place Marcelin Berthelot 75005 Paris, France

³Institute for Advanced Studies in Basic Sciences, Zanjan 45195-159, Iran

We examine whether cubic non-linearities, allowed by symmetry in the elastic energy of a contact line, may result in a different universality class at depinning. Standard linear elasticity predicts a roughness exponent $\zeta = 1/3$ (one loop), $\zeta = 0.388 \pm 0.002$ (numerics) while experiments give $\zeta = 0.5$. Within functional RG we find that a non-local KPZ-type term is generated at depinning and grows under coarse graining. A fixed point with $\zeta = 0.45$ (one loop) is identified, showing that large enough cubic terms increase the roughness. This fixed point is unstable, revealing a rough strong-coupling phase. Experimental study of contact angles near $\theta_c = 2$, where cubic terms in the energy vanish, is suggested.

Experiments measuring the roughness of the contact line of a fluid wetting a disordered solid substrate have consistently found a value $\zeta = 0.5$ for the roughness exponent. This result is highly reproducible from superfluid Helium [1] to viscous glycerol-water mixtures [2], and in situations which can rather convincingly be argued to be at or at least very near the depinning transition. Explaining this high value for ζ poses a theoretical challenge. It may result in a broader understanding of the depinning transition in other systems, since similar values are also measured in cracks [3].

The simplest elastic model of a contact line [4] consists of an effective elastic energy, quadratic in the height field $h(\mathbf{x})$ (displacement in the solid plane), with non-local dispersion $\propto q^2$ (long-range elasticity) due to the surface tension of the fluid meniscus. Substrate inhomogeneities are modeled by a random-field disorder coupling to $h(\mathbf{x})$. The resulting model for the depinning transition of an elastic manifold (generalized to d internal dimensions, here $d = 1$) has been extensively studied, and the predictions debated for some time. Functional RG (FRG) methods were developed initially to one loop [5] predicting $\zeta = 1/3$ to all orders, here $\zeta = 2/d$, identical to the statics of random field. Careful analysis beyond one loop however revealed new irreversible terms in the RG which clearly distinguish statics and depinning, and yield $\zeta = 1/3(1 + 0.397\epsilon) + O(\epsilon^2)$ [6]. Novel high-precision numerical algorithms found [7] $\zeta = 0.388 \pm 0.002$ midway between the one- and two-loop results. This value is too low to account for the experiments.

Various mechanisms have been proposed [8] such as lateral waves or plastic-type dynamics. It is unclear whether any of them are universal enough to explain the robustness of the experimental values for ζ . More complex dissipation mechanism may be at play but they should not be important for the roughness if, as believed [2], the experiment is at quasi-static depinning.

Before abandoning the elastic model, one must first check for neglected effects. It has been known for some time, for conventional linear elasticity $\propto q^2$, that there is another universality class, anisotropic depinning [9, 10, 11]. There, a non-linear Kardar-Parisi-Zhang (KPZ) term $(\nabla h)^2$ becomes relevant, resulting in a singular dependence of the threshold force on rotation of the contact line in the plane. That such a dissipative term is generated in the equation of motion at

velocity $v > 0$ is straightforward, and it was shown recently within the FRG that it survives [12] even at quasi-static depinning $v \rightarrow 0^+$, only if anisotropy exists in the substrate disorder or in the motion of the manifold. Although Ref. [12] shows that a larger exponent is possible for long-range elasticity, an explanation based on this term alone is problematic.

An important feature of the contact-line problem is that at contact angles different from $\theta_c = 2$ the symmetry $h \rightarrow -h$ is absent. Thus the elastic energy contains cubic non-linear and non-local terms. The equation of motion thus contains non-linear terms breaking this symmetry, even in the absence of a driving force [13]. Being different in nature from the conventional dissipative KPZ term, it is important to understand their effect at quasi-static depinning. Their effect in the moving phase has been recently investigated [13], and found to lead to a roughening transition analyzed in connection with the development of a Landau-Levich film.

The aim of this letter is to examine whether non-linear terms in the energy may result in a different universality class at depinning. Although naively irrelevant, they do generate at depinning a *non-local* KPZ-type term which grows under coarse-graining. We find via a FRG calculation two possible phases separated by a fixed point at a critical value of the disorder. Interestingly, the roughness exponent at this critical point is, within one-loop accuracy, $\zeta = 0.45 > 1/3$. Although we do not control the rough phase at strong disorder, this shows that ζ can be increased by non-linear terms. This growing non-local term also arises in the moving phase, with similar features and a significantly smaller exponent. We discuss the interest of studying the system for interfaces with contact angles in the vicinity of $\theta_c = 2$, the point where cubic terms in the energy vanish.

Let us describe the model of Ref. [4, 13] for a fluid wetting a flat solid in coordinates suitable for any (global) equilibrium contact angle $\theta_c = \theta_e$, see Fig. 1. The liquid-air interface (LA) is denoted by $\mathbf{f}(\mathbf{x}; y; z(\mathbf{x}; y))$ (flat when $z(\mathbf{x}; y) = 0$), the flat solid (S) surface by $\mathbf{f}(\mathbf{x}; y; y \tan \theta_e)$. They meet at the contact line $y = h(\mathbf{x}) \cos \theta_e$, included in (S), the boundary condition $z(\mathbf{x}; y = h(\mathbf{x}) \cos \theta_e) = h(\mathbf{x}) \sin \theta_e$. The total energy is $E = E_{LA} + E_{SL}$ with:

$$E_{LA}[z] = \int_{LA} d\mathbf{x} \int_{y > h(\mathbf{x}) \cos \theta_e}^z dz \mathcal{A}[z(\mathbf{x}; y)] \quad (1)$$

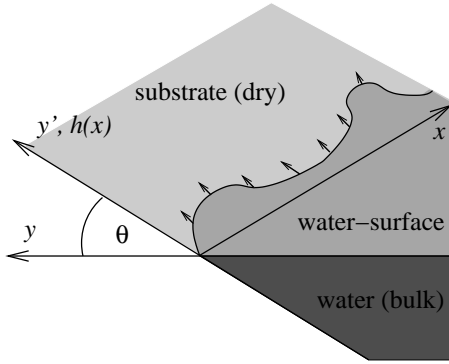


FIG. 1: The geometry of the contact-line.

$$E_{SL} = \int_{y^0 > h(x)} dx \int dy^0 (\mathbf{x}; y^0); \quad (2)$$

where $A = \frac{1}{1 + (\partial_x z)^2 + (\partial_y z)^2}$ gives the LA area, and the wetting area energy density $\gamma_{SL} = \gamma_{AS}$ is a random function of the in-plane position ($y^0 = y \cos \theta$). Minimizing the

LA interface energy E_{LA} for fixed $h(\mathbf{x})$ yields the equilibrium profile $z_h(\mathbf{x}; y)$, and one can show that the relation between force and contact angle holds locally, $E_{LA}[z_h] = h(\mathbf{x}) = \gamma_{LA} \cos \theta(\mathbf{x})$. One defines the equilibrium contact-angle value θ_e via the average force, i.e. through $\langle \mathbf{x}; y^0 \rangle = \gamma_{LA} \cos \theta_e + \langle \mathbf{x}; y^0 \rangle$ with $\langle \mathbf{x}; y^0 \rangle = 0$.

Expansion of $E_{LA}[z_h]$ up to third order in h proceeds by solving $\nabla^2 z_h = 0$ in the form $z_h(\mathbf{x}; y) = \sum_{\mathbf{q}} c_{\mathbf{q}} e^{i\mathbf{q}\cdot\mathbf{x}} \frac{y}{h_0}$. Solving for the boundary conditions and inserting in $E_{LA}[z_h]$ yields, up to terms of $O(h^4)$:

$$E_{LA}[h] = \frac{c_1}{2} \int_{\mathbf{q}} h_{\mathbf{q}} h_{-\mathbf{q}} + \frac{c_2}{2} \int_{\mathbf{q}, \mathbf{k}} [i\mathbf{q} \cdot \mathbf{k} + c_3] h_{\mathbf{k}} h_{\mathbf{q}} h_{-\mathbf{q}-\mathbf{k}} \quad (3)$$

with $c_1 = \sin^2(\theta_e)$, $c_2 = c_3 \cos(\theta_e)$. The form of the cubic term $e_{c_1, c_2, c_3} h_{\mathbf{q}_1} h_{\mathbf{q}_2} h_{\mathbf{q}_3}$, $c_i = 0$, with $e_{c_1, c_2, c_3} = \int_{\mathbf{q}_1, \mathbf{q}_2, \mathbf{q}_3} c_i(\mathbf{q}_1, \mathbf{q}_2, \mathbf{q}_3)$ is the only possibility imposing that e is symmetric, homogeneous of degree 2, and vanishes for $c_1 = 0$ (invariance under a uniform shift $h(\mathbf{x}) \rightarrow h(\mathbf{x}) + \text{const}$). As expected the symmetry $h_{\mathbf{k}} \rightarrow h_{-\mathbf{k}}$ is restored for $\theta_e = \pi/2$ where $c_1 = 0$. To the same order the general form of the equation of motion (EOM) is:

$$\partial_t h_{\mathbf{k}; t} = c(\mathbf{k}) h_{\mathbf{k}; t} - \frac{1}{2} \int_{\mathbf{q}} [c_2(\mathbf{q}; \mathbf{k} - \mathbf{q}) + c_3(\mathbf{k}; \mathbf{q}) + c_3(\mathbf{k}; \mathbf{k} - \mathbf{q})] h_{\mathbf{q}; t} h_{\mathbf{k} - \mathbf{q}; t} + \int_{\mathbf{x}} [F(\mathbf{x}; h(\mathbf{x}) + vt) + f(\mathbf{x})] e^{i\mathbf{k}\cdot\mathbf{x}} \quad (4)$$

where the pinning force has correlator $\overline{F(\mathbf{x}; h) F(\mathbf{x}^0; h^0)} = \delta(\mathbf{x} - \mathbf{x}^0) (h - h^0)$, and a thermal noise may be added. In view of later RG calculations, we slightly generalize the model, defining (with normalized vectors $\hat{\mathbf{q}} = \mathbf{q}/|\mathbf{q}|$):

$$c_i(\mathbf{q}_1; \mathbf{q}_2) = \int_{\mathbf{p}_1, \mathbf{p}_2} f_i(\hat{\mathbf{q}}_1 - \hat{\mathbf{q}}_2); \quad c(\mathbf{q}) = c \int_{\mathbf{p}} \quad (5)$$

The contact line corresponds to $\theta_e = 1$. For reasons detailed below we consider the parameterization:

$$f_2(z) = c_3(1 + g(z)) + c_0; \quad f_3(z) = c_3(1 + g(z)) \quad (6)$$

where $g(z) = z$ or more generally an odd function with $g(1) = 1$. This EOM is obtained from (3) in the simplest case, which assumes fast relaxation of the meniscus and dissipation via molecular jumps [13, 16]:

$$\frac{\partial_t h(\mathbf{x}; t)}{1 + (\partial_x h)^2} = \frac{E[h]}{h(\mathbf{x}; t)} = [c \cos \theta(\mathbf{x}; t) - c \cos \theta_e] + \langle \mathbf{x}; h(\mathbf{x}; t) \rangle; \quad (7)$$

where c is a dissipative coefficient (note that the above equation neglects viscous hydrodynamic losses inside the moving liquid wedge [17]).

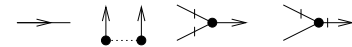
At zero or vanishingly small velocity, i.e. at the depinning threshold, the non-linearity $(\partial_x h)^2$ on the left-hand side can be neglected to this order, and using the form (3) one finds (4) and (6) with $c_3 = c$, $c_0 = 0$ and $F(\mathbf{x}; h) = \langle \mathbf{x}; h \rangle$. These are the microscopic (bare) values, and we show below that the form given in (5) and (6) is preserved under RG at

depinning. The crucial point is that, while forbidden at the bare level by the potential form of the EOM $\partial_t h = E[h]$, a non-zero and positive value for c_0 will be generated *beyond the Larkin length* from the non-analyticity of the renormalized force correlator. It corresponds to the generation of a *non-local* KPZ-type term. The case of more complicated dynamics is mentioned below. We now focus on the analysis of (4).

FRG starts by calculating the 1-loop corrections to (4) and its associated dynamical action, perturbatively in (h) and the c_i . Graphical rules are given in Fig. 2. The graphs representing the corrections to c , c_i , (h) and $\langle \mathbf{x}; h \rangle$ are shown in Fig. 3. To illustrate the main ideas, we explain how the first correction to c is computed. It is the sum of two contributions (see Fig. 4):

$$c(p) = \frac{c_0(0^+)}{c^2} \int_{\mathbf{k}} \frac{\mathbf{k} \cdot \mathbf{p}}{\mathbf{k}^2 + \mathbf{p}^2} f_2(\hat{\mathbf{k}} - \hat{\mathbf{p}}) + \frac{\mathbf{p} \cdot \mathbf{p}}{\mathbf{k}^2} f_3(\hat{\mathbf{p}} - \hat{\mathbf{q}}); \quad (8)$$

where $\mathbf{q} = (\mathbf{p} + \mathbf{k})$. These are depicted on Fig. 4 in the order of their appearance in (8). Denominators originate from time integrals of the bare response $R_{\mathbf{k}; t} = \langle \mathbf{x} \rangle^1 e^{c \int_{\mathbf{k}} \mathbf{k} \cdot \mathbf{p} t} (t)$,

FIG. 2: The graphical rules: Propagator, disorder vertex, non-linearity γ_2 and non-linearity γ_3 .

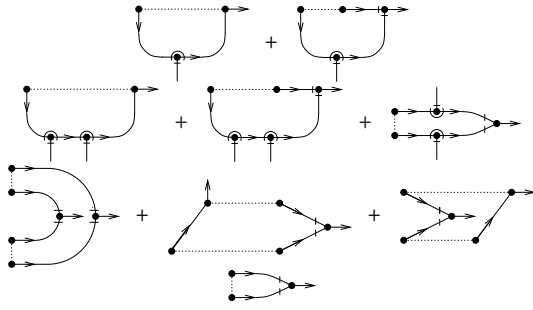


FIG. 3: The diagrams correcting c (first line), ϵ_1 (second line), \tilde{h} (third line) and \tilde{c} (last line). Only diagrams proportional to ϵ_1 are shown.

while numerators come from the cubic vertices. The factor $\epsilon_1(0^+)$ is $\epsilon_1(v(t-t^0))$, taken in the limit of $v \rightarrow 0^+$ and is non-vanishing only when the cusp is formed, i.e. beyond the Larkin length. Expanding in vanishing external momentum p yields:

$$c = \frac{\epsilon_1(0^+)}{c^2} \frac{1}{k} \frac{1}{j} \text{hf}_2(z) + f_3(z) \epsilon_1; \quad (9)$$

where $\text{hf}(z)$ denotes the angular average $\frac{R_1}{1} dz$ (z^2) $\frac{d-3}{2} f(z)$ (with $\text{hf}_1 = 1$). Appearance of the combination $\text{hf}_2(z) + f_3(z) \epsilon_1 = 2\epsilon_3 + \epsilon_0$ for arbitrary odd $g(z)$ in all graphs is a general feature and yields the (re)definition of the vertex explained in Fig. 4. It gives the “anomalous” correction (i.e. resulting from the cusp) to c to which the second one of Fig. 3 must be added. One shows that there is no correction to the non-linear vertex function $f_3(z)$ because that would involve necessarily another f_3 vertex with an external h leg at zero external momentum, yielding $f_3(1) = 0$ (which remains true since there is no mechanism to correct it). Thus one finds $\epsilon_3 = 0$. In the graphs correcting f_2 (second line of Fig. 3) appearance of the above-mentioned combination implies that only the uniform part of f_2 , i.e. ϵ_0 is corrected:

$$\epsilon_0 = (2\epsilon_3 + \epsilon_0)^2 - 2 \frac{\epsilon_1(0^+)}{c^3} \frac{1}{k} + 3 \frac{\epsilon_1(0)}{c^4} \epsilon_0; \quad (10)$$

While in standard (thermal) KPZ the two corresponding diagrams have opposite sign because of the derivatives and is uncorrected (a consequence of Galilean invariance), here the presence of *absolute values* of the momenta results in the same sign.

Corrections to disorder (line 3 of Fig. 3) are the same as in [12]. Power counting then leads to the definitions $\tilde{h}(h) = \frac{d-2}{2} c^2 \tilde{h}(h)$, $\tilde{\epsilon}_1 = \frac{1}{c} \epsilon_1$, where $\epsilon_1 = e^1$ is the running UV cutoff (e.g. in a Wilson approach). One finally obtains the following set of FRG equations (with $\epsilon =$

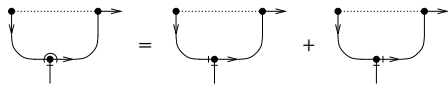


FIG. 4: The first diagram from Fig. 3 correcting c , see (8).

2 d):

$$\begin{aligned} \epsilon_1 \ln c &= \epsilon_1(0^+) (2\epsilon_3 + \epsilon_0) - \epsilon_1(0) (2\epsilon_3 + \epsilon_0) \epsilon_0 \\ \epsilon_1 \ln \tilde{\epsilon}_3 &= \epsilon_1 \ln c \\ \epsilon_1 \tilde{\epsilon}_0 &= (\epsilon_1 \ln c) \tilde{\epsilon}_0 - 2\epsilon_1(0^+) (2\epsilon_3 + \epsilon_0)^2 \\ &\quad + 3\epsilon_1(0) \tilde{\epsilon}_0 (2\epsilon_3 + \epsilon_0)^2 \\ \epsilon_1 \tilde{h}(h) &= (2\epsilon_1 \ln c) \tilde{h}(h) + h \epsilon_1(0) \tilde{h}(h) \\ &\quad + \frac{1}{2} \tilde{h}(h)^2 \tilde{\epsilon}_0^2 [\epsilon_1(0) \tilde{h}(h)^2 + \epsilon_1(0) \tilde{h}(h) \tilde{h}(h) - \epsilon_1(0)] \\ \epsilon_1 \ln \tilde{c} &= \frac{1}{2} \epsilon_1(0^+) \tilde{\epsilon}_0 - \epsilon_1(0) \tilde{c} : \end{aligned} \quad (11)$$

They admit the standard attractive depinning fixed point corresponding to linear elasticity (isotropic IS depinning class): $\tilde{\epsilon}_3 = \tilde{\epsilon}_0 = 0$ and $\tilde{h}_{IS}(h)$ with $\tilde{c} = 3$ to this order (corrected at two loops). To order ϵ_1 , this FP is stable to adding a small non-zero $\epsilon_3; \epsilon_0$ which have linear eigenvalue ϵ_1 . This FP controls a phase with small ϵ_0 and ϵ_3 . ϵ_0 is generated from ϵ_3 beyond the Larkin length and the ratio $\epsilon_0 = \epsilon_3$ goes to a constant in this phase.

We found a second fixed point which controls at given disorder the transition between the small $\tilde{\epsilon}_0$ phase and a large $\tilde{\epsilon}_0$ regime (strong coupling). One easily sees that the ratio $\tilde{\epsilon}_3 = \tilde{\epsilon}_0$ flows to zero at this transition. To look for the FP one can thus set $\tilde{\epsilon}_3 = 0$ and redefine $\hat{h}(h) = \tilde{\epsilon}_0 \tilde{h}(h)$, yielding:

$$\begin{aligned} \epsilon_1 \hat{h}(h) &= [2\hat{h}^2 - 2\hat{h}(0^+) + 2\hat{h}(0)] \hat{h}(h) + \hat{h} \hat{h}(0) \\ &\quad + \frac{1}{2} \hat{h}(h)^2 [\hat{h}(0)^2 + \hat{h}(0) \hat{h}(h) - \hat{h}(0)] \end{aligned} \quad (12)$$

with $\epsilon_1 \ln \tilde{\epsilon}_0 = \hat{h}$ and $\hat{c} = 3\hat{h}(0^+) - 4\hat{h}(0)$. The FP function obtained numerically $\hat{h}(h) = \hat{f}_a(h)$ is positive and short-ranged, and \hat{f}_a depends only on $a = \epsilon_1$; the associated roughness exponent is

$$\epsilon_1 = 0.450512 \quad (13)$$

for $a = 1$, which should be compared to the value $\epsilon_{IS} = 3$ to the same 1-loop accuracy, demonstrating the increase in the roughness exponent due to non-linearities. If we assume the same relative increase of ϵ_1 due to the higher-loop corrections [6] from $\epsilon_{IS} = 0.388$ to 0.002 [7], we would obtain here $\epsilon_1 = 0.53$, tantalizingly close to the experiments. The dynamical exponent is $z = 1 + \epsilon_1 \ln(\epsilon_1)$, i.e. $z = 1.0205213$ yielding $z = 0.79487$ for the physical case. As for anisotropic depinning, a third exponent is necessary here, $\epsilon_1 \ln c = 0.170449$, and scaling yields the correlation length exponent $\nu = 1/(z + \epsilon_1)$ and the velocity-force exponent $\nu = (z + \epsilon_1) \epsilon_1 = 0.478$ such that $\nu = (\epsilon_1 - \epsilon_c)$. This fixed point is unstable in one direction (leading eigenvalues $\epsilon_1 = 0.938$ and $\epsilon_2 = 1.23$) consistent with the existence of two phases. The strong-coupling phase cannot be accessed by the present method, but the increase of ϵ_1 is likely to persist there. Since this FP is attractive in all other directions the experiments may be susceptible to a very long crossover dominated by this FP. This can be tested by careful numerical integration of (11), not attempted here.

The FRG equations (11) have been derived within a double expansion in ϵ_1 and ϵ_1 . The question arises of

whether operators with more non-local derivatives $\nabla^2 h$ are indeed irrelevant, as suggested by power-counting. A detailed analysis shows that in the space of perturbations where one adds to (h_{xt}, h_{xt^0}) the two functions $\nabla^2 h_{xt}, \nabla^2 h_{xt^0}$ ($\nabla^2 h_{xt} + \nabla^2 h_{xt^0}$) + $\nabla^2 h_{xt}, \nabla^2 h_{xt^0}$ ($\nabla^2 h_{xt} - \nabla^2 h_{xt^0}$), the largest eigenvalue is 0 ± 2 (for $\nu = 1$), indicating no additional instability of the FP. These terms arise at the bare level for a more complicated dynamics, but should not change the result in the quasi-static limit studied here [14].

We now sketch the analysis of the moving case, very near depinning, $\nu > 0$ small, for details see [14]. Since the generation of ϕ_0 is a new feature, we reexamine [13]. At large scales in the moving phase the quenched pinning force acts as a (thermal) white noise of strength $2D$ (notation as in [13]) and thus ϕ_0 is uncorrected. Using the same parameterization as above we find [15]:

$$\begin{aligned} \partial_1 \ln \epsilon &= z - \frac{1}{4}g(1+2r) \\ \partial_1 \ln \tilde{\epsilon}_0 &= z + \frac{1}{2} + \frac{1}{4}g(1+2r)^2 \\ \partial_1 g &= (d+1)g + g^2 \frac{1}{8} + \frac{3}{4}(1+2r) + \frac{1}{2}(1+2r)^2 \end{aligned} \quad (14)$$

with $\partial_1 \ln r = \frac{1}{4}g(1+2r)^2$ and we have defined $\epsilon = c_1 z$, $\tilde{\epsilon}_i = \epsilon_1^2 (z+1)$ ($i = 0, 3$), $\tilde{D} = D_1^{d+2} z$, $g = \epsilon^3 \tilde{D}^2$, and $r = \tilde{\epsilon}_3 / \tilde{\epsilon}_0$. These equations exhibit a

weak-coupling phase controlled by the $g = 0$ attractive fixed point (which, in the physical case corresponds to logarithmic roughness $\phi_0 = 0$) and a strong-coupling phase. They are separated by a FP at $g = g^* = \frac{8}{11}(d+1)$, with *universal* values for the exponents $z = \frac{1}{2} + \frac{2}{11}(d+1)$ and $\phi_0 = \frac{d}{2} + \frac{3}{11}\frac{d+1}{2}$, i.e. for $d = 1$:

$$0.273 \leq z \leq 1.364 \quad (15)$$

This rather low value for ϕ_0 suggests that a scenario based on a slowly moving contact line is not adequate to explain the experimentally observed roughness.

In conclusion, we have examined using RG the effect of non-linear elasticity for the contact line at and near depinning. We found that even for isotropic disorder, a non-local KPZ term is generated and may, for large enough bare non-linear elasticity and disorder, destabilize the standard linear-elasticity depinning fixed point, yielding values for the roughness exponent compatible with experiments. This scenario could be tested by high-precision numerics. It may also be explored experimentally by carefully choosing the fluid and the solid substrate [18]: since all odd non-linear terms in the elastic energy vanish at $\nu = 2$ one can surmise that the total effect of non-linear terms, and hence the apparent contact-line roughness, is minimal there [19].

We thank C. Guthmann, W. Krauth, S. Moulinet, E. Rolley, A. Rosso and T. Vilmin for interesting discussions.

-
- [1] A. Prevost, E. Rolley, C. Guthmann, Phys. Rev. B **65**, 064517 (2002).
 - [2] S. Moulinet, C. Guthmann and E. Rolley, Eur. Phys. J. E **8**, 437 (2002). S. Moulinet et al., Phys. Rev. E **69**, 035103 (2004).
 - [3] A. Deleplace et al., Phys. Rev. E **60**, 1337 (1999).
 - [4] J.F. Joanny and P.G. De Gennes, J. Chem. Phys. **81**, 552 (1984).
 - [5] D. Ertas and M. Kardar, Phys. Rev. E **49**, 2532 (1994).
 - [6] P. Chauve, P. Le Doussal and K.J. Wiese, Phys. Rev. Lett. **86**, 1785 (2001). P. Le Doussal, K.J. Wiese and P. Chauve, Phys. Rev. B **66**, 174201 (2002).
 - [7] A. Rosso and W. Krauth, Phys. Rev. E **65**, R025101 (2002).
 - [8] E. Bouchaud et al., J. Mech. Phys. Solids **50**, 1703 (2002).
 - [9] L.A.N. Amaral, A. Barabasi and H.E. Stanley, Phys. Rev. Lett. **73**, 62 (1994).
 - [10] A. Rosso and W. Krauth, Phys. Rev. Lett. **87**, 187002 (2001).
 - [11] L.-H. Tang, M. Kardar and D. Dhar, Phys. Rev. Lett. **74**, 920 (1995).
 - [12] P. Le Doussal and K.J. Wiese, Phys. Rev. E **67**, (2003) 016121.
 - [13] R. Golestanian and E. Raphael, Europhys. Lett. **55**, 228 (2001); Erratum, Europhys. Lett. **57**, 304 (2002); Phys. Rev. E **67**, 031603 (2003).
 - [14] P. Le Doussal, K.J. Wiese, E. Raphael, R. Golestanian, unpublished.
 - [15] Additional non-potential terms appearing at $\nu > 0$ are found to be irrelevant (as compared to ϕ_0) if ν is small enough, hence (14) is restricted to small ν .
 - [16] T. Blake in *AICHE International Symposium on the mechanics of thin film coating* (New Orleans, 1988).
 - [17] P.G. de Gennes, Rev. Mod. Phys. **57**, 827 (1985).
 - [18] P.-G. de Gennes et al., *Capillarity and Wetting Phenomena: Drops, Bubbles, Pearls, Waves* (Springer, 2003).
 - [19] Perturbative calculations [14] show that even for $\nu = 2$ a smaller but positive ϕ_0 term is generated from fourth order non-linear elasticity beyond the Larkin Length.